positions suggests the C2–C1–O5–C6 part of these glycosides sits directly upon, or slightly into, the phosphocholine surface. One must, of course, remember that in both the case of DMPC and the case of the glycoside we are dealing with highly averaged structures.[52,53]

Thus, we have been able to build a generally coherent picture of the average conformation and orientation of a series of simple glycosides at a membrane interface. The series suggests the importance of some hydrophobic interactions at the membrane interface in addition to the more often cited hydrogen-bonding interactions. It would appear that extension of the specific developments reported herein to a wider class of molecules and to more biologically relevant structures would be possible. If so, it should be possible to build a sound physical basis for understanding the interactions of glycolipids with membrane components.

Acknowledgment. We thank Brian Hare and Kathleen Howard for their generous assistance in running computations and Yves Aubin for synthesizing β-dodecyl galactose. Dr. Yuying Gosser is acknowledged for her work on interpretation of chemical shift anisotropy effects. Support for this work was provided by the NIH Grant GM33225. C.R.S. was supported by NIH Fellowship GM 13227.

(53) DeLoof, H.; Harvey, S.; Segrest, J.; Pastor, R. *Biochemistry* **1991**, *30*, 2099–2113.

Structure of the Radical Cations of *N,N'*-Polymethylene-*syn*-1,6:8,13-diimino[14]annulenes: An ESR and ENDOR Study

Fabian Gerson,*,† Georg Gescheidt,† Jürgen Knöbel,†,§ William B. Martin, Jr.,†,⊥ Ludger Neumann,‡ and Emanuel Vogel‡

Contribution from the Institut für Physikalische Chemie der Universität Basel, Klingelbergstrasse 80, CH-4056 Basel, Switzerland, and Institut für Organische Chemie der Universität Köln, Greinstrasse 4, D-5000 Köln 41, FRG. *Received March 6, 1992*

Abstract: *N,N'*-Polymethylene-*syn*-1,6:8,13-diimino[14]annulenes, **1–7**, in which the number, *m*, of CH_2 groups varies from 1 to 7, and *N,N'*-dimethyl-*syn*-1,6:8,13-diimino[14]annulene (**8**) were synthesized. The radical cations of **1–8**, as well as those of several derivatives of **1–4**, have been studied by ESR, ENDOR, and TRIPLE resonance spectroscopy. In contrast to the corresponding anions $\mathbf{1}^{\bullet-}$–$\mathbf{8}^{\bullet-}$, which are bridged π-perimeter radicals, the cations $\mathbf{1}^{\bullet+}$–$\mathbf{8}^{\bullet+}$ must be considered as N-centered radicals with the bulk of the spin population residing at the two heteroatoms. The structure and properties of these radical cations critically depend on the length of the polymethylene chain linking the N atoms. When the number, *m*, of the CH_2 groups in this chain is 1 or 2, the N lone pairs are directed "outward", so that their interaction is relatively weak. Thus, the radical cations $\mathbf{1}^{\bullet+}$ (m = 1) and $\mathbf{2}^{\bullet+}$ (m = 2) are thermodynamically and kinetically rather unstable, and their ^{14}N coupling constant, a_N, is only 0.6–0.7 mT. On the other hand, with m = 3–7 the N lone pairs point "inward", an arrangement that favors the formation of an N–N three-electron σ-bond. The pertinent radical cations $\mathbf{3}^{\bullet+}$–$\mathbf{7}^{\bullet+}$ (m = 3–7) exhibit unusual thermodynamic and kinetic stabilities which, in two cases ($\mathbf{3}^{\bullet+}$ and $\mathbf{4}^{\bullet+}$), allowed X-ray crystallographic structure analyses to be carried out. The coupling constant a_N amounts to 1.70 mT for $\mathbf{3}^{\bullet+}$, and it increases further to an almost constant value of 2.57–2.72 mT for $\mathbf{4}^{\bullet+}$–$\mathbf{7}^{\bullet+}$; an a_N value of 2.66 mT is also observed for $\mathbf{8}^{\bullet+}$, which may be regarded as having its N atoms linked by a very long polymethylene chain. The changes in the coupling constant a_N along the $\mathbf{1}^{\bullet+}$–$\mathbf{7}^{\bullet+}$ ($\mathbf{8}^{\bullet+}$) series can be rationalized in terms of the varying "s-character" of the singly occupied orbital centered at the spin-bearing N atoms.

Introduction

Derivatives of *syn*-1,6:8,13-diimino[14]annulene,[1,2] in which a polymethylene chain links the two N atoms, are ideal models for the studies of the interaction between such nonbonded but spatially close atoms. That is because the geometry and electronic structure of the N atoms in these derivatives can systematically be modified by varying the number of the CH_2 groups in the linking chain. The corresponding radical cations are particularly suitable for the studies in question, as ionization can lead to the formation of an N–N three-electron σ-bond[3-7] and as the unpaired spin is appropriate to probe the N–N interaction.[3b,4-6]

The present paper deals with ESR and ENDOR investigations on the radical cations of several *N,N'*-alkanediyl-*syn*-1,6:8,13-diimino[14]annulenes where alkanediyl is methylene (**1**), perdeuteriomethylene (**1**-d_2), isopropylidene (**1**-Me_2), perdeuterioisopropylidene (**1**-$(CD_3)_2$), dimethylene (**2**), perdeuteriodimethylene (**2**-d_4), trimethylene (**3**), 2,2-dideuteriotrimethylene (**3**-d_2), tetramethylene (**4**), 2,2,3,3-tetradeuteriotetramethylene

* Author to whom correspondence should be addressed.
† Universität Basel.
‡ Universität Köln.
§ Present address: F. Hoffmann-La Roche AG, CH-4058 Basel, Switzerland.
⊥ Professor Emeritus, Department of Chemistry, Union College, Schenectady, NY 12309.

(1) (a) Vogel, E.; Kuebart, F.; Marco, J. A.; Andrée, R.; Günther, H.; Aydin, R. *J. Am. Chem. Soc.* **1983**, *105*, 6982. (b) Destro, R.; Pilati, T.; Simonetta, M.; Vogel, E. *J. Am. Chem. Soc.* **1985**, *107*, 3185.

(2) (a) Vogel, E. *Lect. Heterocycl. Chem.* **1985**, *8*, 103. Andrée, R. Dissertation, Universität Köln, Germany, 1985. Becker, D. Diplomarbeit, Universität Köln, Germany, 1985. (b) Destro, R.; Pilati, T.; Simonetta, M.; Vogel, E. *J. Am. Chem. Soc.* **1985**, *107*, 3192. (c) Wolfrum, P. Dissertation, Universität Köln, Germany, 1990. (d) Houriet, R.; Feng, W.; Vogel, E.; Wolfrum, P.; Schwarz, H. *Int. J. Mass. Spectrom. Ion Processes* **1989**, *91*, R1.

(3) (a) Alder, R. W. *Acc. Chem. Res.* **1983**, *16*, 321 and references therein. (b) Kirste, B.; Alder, R. W.; Sessions, R. B.; Bock, M.; Kurreck, H.; Nelsen, S. F. *J. Am. Chem. Soc.* **1985**, *107*, 2635. (c) Alder, R. W.; Orpen, A. G.; White, J. M. *J. Chem. Soc., Chem. Commun.* **1985**, 949.

(4) Gerson, F.; Knöbel, J.; Buser, U.; Vogel, E.; Zehnder, M. *J. Am. Chem. Soc.* **1986**, *108*, 3781.

(5) Gerson, F.; Gescheidt, G.; Buser, U.; Vogel, E.; Lex, J.; Zehnder, M.; Riesen, A. *Angew. Chem., Int. Ed. Engl.* **1989**, *28*, 902.

(6) Dinnoncenzo, J. P.; Banach, T. E. *J. Am. Chem. Soc.* **1988**, *110*, 971.

(7) For theoretical work, see: Bouma, W. J.; Radom, L. *J. Am. Chem. Soc.* **1985**, *107*, 345. Gill, P. M. W.; Radom, L. *J. Am. Chem. Soc.* **1988**, *110*, 4931.

0002-7863/92/1514-7107$03.00/0

Table I. Half-Wave Oxidation Potentials $E_{1/2}$ (vs SCE) of the Parent *syn*-1,6:8,13-Diimino[14]annulene and Its Derivatives **1**–**8** and **1**-Me_2[a]

compd	$E_{1/2}$, V	compd	$E_{1/2}$, V
parent	(+0.78)[b]	**4**	+0.29
1	+0.78	**5**	+0.22
1-Me_2	+0.85	**6**	+0.61
2	(+0.90)[b]	**7**	+0.51
3	+0.24	**8**	+0.42

[a] Experimental error: ±0.01 V. [b] Irreversible wave; the value refers to the oxidation peak E_p.

(**4**-d_4), pentamethylene (**5**), hexamethylene (**6**), and heptamethylene (**7**). The notation **1**–**7** refers to the number, m = 1–7, of CH_2 groups in the chain linking the two N atoms. Also investigated are the radical cations of **3**-Br, the 2-bromo derivative of **3**, and of *N*,*N*′-dimethyl-*syn*-1,6:8,13-diimino[14]annulene (**8**).

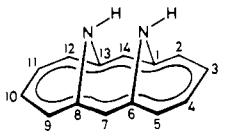

syn-1,6:8,13-Diimino[14]annulene

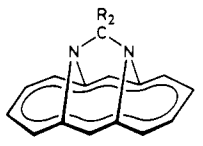

1 R=H **1**-Me_2 R=CH_3
1-d_2 R=D **1**-$(CD_3)_2$ R=CD_3

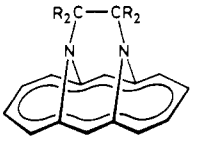

2 R=H **2**-d_4 R=D

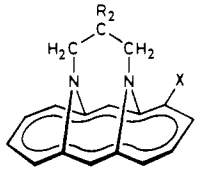

3 R=X=H **3**-d_2 R=D, X=H
3-Br R=H, X=Br

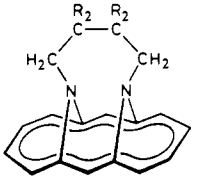

4 R=H **4**-d_4 R=D

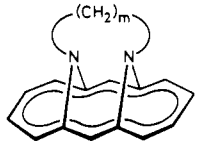

5 m=5 **6** m=6 **7** m=7

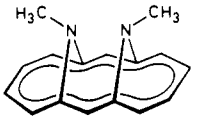

8

Some ESR spectroscopic data for $3^{\bullet+}$ and $4^{\bullet+}$ have been previously reported,[4,5] along with the X-ray crystallographic structures of their ClO_4^- salts. The two diimino[14]annulenes **3** and **4** as well as diazabicyclo[4.4.4]tetradecane (**9**)[3c] represent, to our knowledge, the only molecular species for which the formation of an N–N three-electron σ-bond upon ionization has been established by X-ray crystallography.

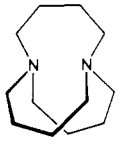

9

Results

Table I lists the oxidation potentials measured by cyclic voltammetry for *syn*-1,6:8,13-diimino[14]annulene and its derivatives **1**, **1**-Me_2, and **2**–**8** in a 0.1 N solution of tetraethylammonium tetrafluoroborate at ambient temperature (working electrode, platinum disc; counter electrode, platinum wire; auxiliary electrode, Ag/AgCl; scan, 200 mV/s). The ease of formation (thermodynamic stability) of the corresponding radical cations thus increases in the following order: (parent diimine)$^{\bullet+}$, $\mathbf{1}^{\bullet+}$, **1**-$Me_2^{\bullet+}$, $\mathbf{2}^{\bullet+}$ < $\mathbf{6}^{\bullet+}$, $\mathbf{7}^{\bullet+}$, $\mathbf{8}^{\bullet+}$ < $\mathbf{3}^{\bullet+}$, $\mathbf{4}^{\bullet+}$, $\mathbf{5}^{\bullet+}$. Except for the parent diimine and **2**, all oxidation waves exhibit reversible behavior under the applied experimental conditions, yielding "true" half-wave potentials $E_{1/2}$. Hence, with these two exceptions, the corresponding radical cations should be persistent (kinetically stable) enough to allow ESR and ENDOR studies over a considerable range of the temperature.

The thermodynamic and kinetic stabilities of the radical cations, as indicated by cyclic voltammetry, are reflected in their properties when prepared for ESR and ENDOR studies. Both electrolytical and "chemical" oxidation methods were used for that purpose, with dichloromethane serving throughout as the solvent. Electrolysis was carried out on a helical gold anode in a cylindric cell with a platinum wire cathode in the cell axis (supporting salt, tetra-*n*-butylammonium perchlorate).[8] Chemical oxidation made use of various reagents, such as tris(*p*-bromophenyl)ammoniumyl hexachloroantimonate, lead tetracetate, nitrosyl tetrafluoroborate, and silver perchlorate. In some experiments, trifluoroacetic acid was added to the solution. Interestingly, Lewis acids, such as $SbCl_5$ and $AlCl_3$, which proved to be very efficient in converting unsaturated hydrocarbons into their radical cations,[9] failed to oxidize *syn*-1,6:8,13-diimino[14]annulene and its derivatives **1**, **1**-Me_2, and **2**–**8**.

The radical cation of the parent diimine had too short a lifetime for a reliable spectroscopic study; it will not be dealt with further in the present paper. The remaining radical cations are reasonably classified as L and M according to their thermodynamic and kinetic stabilities. Class L (*l*ess stable) consists of $\mathbf{1}^{\bullet+}$, **1**-$Me_2^{\bullet+}$, and $\mathbf{2}^{\bullet+}$, while class M (*m*ore stable) comprises $\mathbf{3}^{\bullet+}$–$\mathbf{8}^{\bullet+}$. The radical cations of class L could not be generated by silver perchlorate. Two of them, $\mathbf{1}^{\bullet+}$ and **1**-$Me_2^{\bullet+}$, were stable below ca. 260 K; the third one, $\mathbf{2}^{\bullet+}$, had already decayed above 200 K. The radical cations of class M were generated by any of the methods and reagents mentioned above and persisted up to relatively high temperatures (300–400 K). Perchlorate salts of $\mathbf{3}^{\bullet+}$, $\mathbf{4}^{\bullet+}$, and $\mathbf{8}^{\bullet+}$ were readily isolated, with those of $\mathbf{3}^{\bullet+}$ and $\mathbf{4}^{\bullet+}$ being sufficiently stable for an X-ray crystallographic structure analysis.[4,5]

In the following, the ESR and ENDOR spectra are described for the individual radical cations, which are characterized by their ^{14}N and proton coupling constants, a_N and a_H, respectively. The latter are denoted $a_{H\mu}$ for protons at the centers μ of the 14-membered π-perimeter and $a_{H\beta}$ or $a_{H\gamma}$ for those in the *N*,*N*′-alkanediyl or alkyl groups where β and γ refer to protons separated from the nearest N atom by one and two sp^3-hybridized C atoms, respectively.

***N*,*N*′-Methylene- (1), *N*,*N*′-Isopropylidene- (1-Me_2), and *N*,*N*′-Dimethylene-*syn*-1,6:8,13-diimino[14]annulene (2).** A common feature of $\mathbf{1}^{\bullet+}$, **1**-$Me_2^{\bullet+}$, and $\mathbf{2}^{\bullet+}$ is the grouping of the ESR spectra, due to the coupling constant, a_N, of the two ^{14}N nuclei (0.6–0.7 mT). These spectra are exemplified by that of $\mathbf{1}^{\bullet+}$ shown in Figure 1, together with the corresponding ^{14}N and proton ENDOR spectrum. The proton ENDOR signals occur in pairs at $\nu_H \pm {}^1/_2|a_H|$, where ν_H = 14.56 MHz is the frequency of the free proton and a_H represents the coupling constant in megahertz. This pattern is characteristic of $|a_H|$ being smaller than $2\nu_H$.[10] On the other hand, the ^{14}N ENDOR signals appear at ${}^1/_2|a_N| \pm \nu_N$, because the coupling constant a_N (in megahertz) has an absolute value larger than twice ν_N = 1.05 MHz, the frequency of the free ^{14}N nucleus. The a_N and a_H values used for the simulation of the ESR spectrum are as follows (in millitesla): +0.633 ± 0.005 (2 N), −0.143 ± 0.002 (4 H), and +0.062 ± 0.001 (4 H). Their signs have been determined by the general TRIPLE resonance technique,[10] assuming the a_N value to be positive. The two four-proton values, −0.143 and +0.062 mT, are identified with the coupling constants, $a_{H\mu}$, of perimeter protons, as there is no change in the ESR and ENDOR spectra on passing from $\mathbf{1}^{\bullet+}$ to **1**-$d_2^{\bullet+}$, i.e., on replacing the two methylene β-protons

(8) Ohya-Nishiguchi, H. *Bull. Chem. Soc. Jpn.* **1979**, *52*, 2064.
(9) See, for example: Lewis, I. C.; Singer, L. S. *J. Chem. Phys.* **1965**, *43*, 2712. Gerson, F.; Huber, W.; Lopez, J. *J. Am. Chem. Soc.* **1984**, *106*, 5808.
(10) Kurreck, H.; Kirste, B.; Lubitz, W. *Electron Nuclear Double Resonance Spectroscopy of Radicals in Solution*; VCH Publishers: New York, 1988.

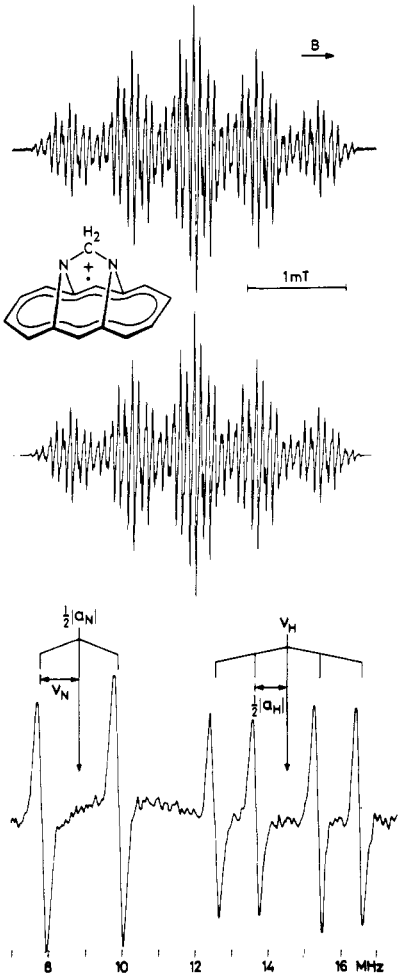

Figure 1. ESR spectrum of $1^{\bullet+}$ (top), its simulation (center), and the corresponding ENDOR spectrum (bottom): solvent, CH_2Cl_2; counterion, $SbCl_6^-$; temperature, 233 K. The simulation of the ESR spectrum made use of the ^{14}N and proton coupling constants given in the text and Table II; line shape Lorentzian, line width 0.015 mT.

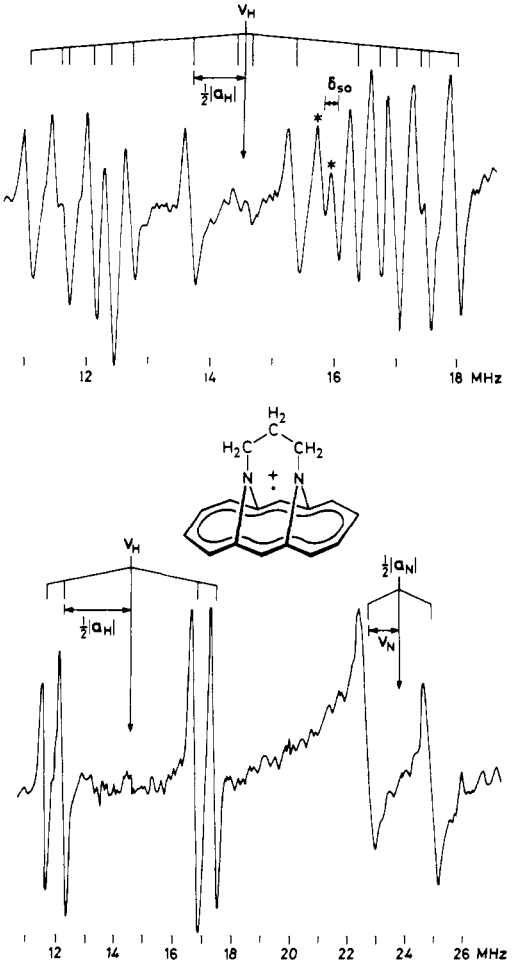

Figure 2. ENDOR spectra of $3^{\bullet+}$: solvent, CH_2Cl_2; counterion, $SbCl_6^-$; temperature, 193 (top) and 243 K (bottom). Note the different frequency scales of the two spectra.

by deuterons. The coupling constant, $a_{H\beta}$, of these protons is thus too small to be observed.

Analogous a_N and a_H values obtained by ESR, ENDOR, and TRIPLE resonance spectroscopy for **1**-$Me_2^{\bullet+}$ are as follows (in millitesla): +0.714 ± 0.005 (2 N), −0.128 ± 0.002 (4 H), +0.106 ± 0.002 (4 H), and 0.014 ± 0.001 (2 H, sign undetermined). Again, all a_H values belong to the perimeter protons ($a_{H\mu}$). The six methyl γ-protons do not give rise to a measurable coupling constant, $a_{H\gamma}$, as the ESR and ENDOR spectra remain unchanged on going from **1**-$Me_2^{\bullet+}$ to **1**-$(CD_3)_2^{\bullet+}$, i.e., on replacing the methyl protons by deuterons.

The same spectroscopic methods applied to $2^{\bullet+}$ yielded the following coupling constants a_N and a_H (in millitesla): +0.611 ± 0.005 (2 N), −0.145 ± 0.002 (4 H), +0.090 ± 0.002 (4 H), and +0.076 ± 0.001 (4 H). Replacement of the four methylene β-protons by deuterons on passing from $2^{\bullet+}$ to **2**-$d_4^{\bullet+}$ causes the disappearance of the coupling constant of +0.090 mT, which thus is identified with $a_{H\beta}$, leaving −0.145 and +0.076 mT for two sets of four perimeter protons ($a_{H\mu}$).

Varying the temperature in the range of 193–298 K has only a little effect on the spectra of $1^{\bullet+}$ and **1**-$Me_2^{\bullet+}$. Corresponding studies could not be carried out for $2^{\bullet+}$, because this radical cation was not persistent above 200 K. Nevertheless, considering that the full symmetry (C_{2v}) of $2^{\bullet+}$ is effective at low temperature, it can safely be assumed that the conformational mobility of the dimethylene chain is not large enough to markedly affect the ESR spectra. As will be shown in the next sections, this behavior contrasts sharply with that of the longer polymethylene chains in $3^{\bullet+}$–$7^{\bullet+}$.

***N,N'*-Trimethylene-*syn*-1,6:8,13-diimino[14]annulene (3).** Due to the conformational inversion of the trimethylene chain (activation energy 28 ± 4 kJ/mol),[4] the ESR and ENDOR spectra of $3^{\bullet+}$ are strongly temperature dependent. The ESR spectrum of $3^{\bullet+}$ at 298 K was reproduced in a previous paper.[4] At that temperature, the rate of inversion is comparable to the hyperfine time scale, and only the sum of two methylene β-proton coupling constants, $|a_{H\beta'} + a_{H\beta''}| = 2.216 \pm 0.020$ mT, was apparent. Other reported data[4] included the ^{14}N coupling constant $|a_N| = 1.685$ ± 0.015 mT, as well as a splitting of 0.180 mT from seemingly eight protons. A more detailed study by ESR, ENDOR, and general TRIPLE resonance spectroscopy has been carried out in the present work. A slow exchange rate is observed below 200 K, while the fast one requires temperatures above 400 K. In between, there is a wide range of intermediate exchange rates which affect the coupling constants of individual protons to different extents.

Figure 2 (top) displays the proton ENDOR spectrum of $3^{\bullet+}$ at 193 K, i.e., at a temperature where the conformational interconversion is frozen. The coupling constants, a_H, determined from the ENDOR signals occurring in pairs at $\nu_H \pm {}^1/_2|a_H|$ are as follows (in millitesla): −0.246 ± 0.002 (1 H), −0.210 ± 0.002 (2 H), −0.203 ± 0.002 (2 H), +0.174 ± 0.002 (2 H), +0.154 ± 0.002 (2 H), −0.129 ± 0.002 (1 H), +0.059 ± 0.001 (2 H), and 0.009 ± 0.001 (1 H, sign undetermined). The signs were again derived from general TRIPLE resonance spectra, assuming that the a_H value of 0.059 mT is positive (see below). In addition to the eight pairs of signals diagnostic of $|a_H| < 2\nu_H$, there are two signals above ν_H with no counterparts below ν_H. The observation of these two signals, separated by only 0.19 ± 0.01 MHz and marked by asterisks in Figure 2, is of some interest, as they are associated with a very large coupling constant ($|a_H| > 2\nu_H$) of two

protons and their separation is due to a second-order splitting (s.o.). To our knowledge, only one report on such a splitting in a proton ENDOR spectrum exists in the literature.[11] The two signals are observed at $^1/_2|a_H| - \nu_H - \delta_{s.o.}$ and $^1/_2|a_H| - \nu_H$ where $\delta_{s.o.}$ is the second-order splitting; their counterparts at $^1/_2|a_H| + \nu_H$ and $^1/_2|a_H| + \nu_H - \delta_{s.o.}$ should appear in the high-frequency range (above 35 MHz), which is not accessible to our ENDOR system. The two protons giving rise to these ENDOR signals are certainly methylene β-protons in a position which favors hyperconjugative interaction with the $2p_z$ AO at the adjacent N atom. The pertinent, undoubtedly positive coupling constant $a_{H\beta'}$ is +2.182 ± 0.008 mT, and the expected second-order splitting[10] is $\delta_{s.o.} = (a_{H\beta'})^2/2B_0$ = 0.007 mT, where B_0 = 0.34 T stands for the magnetic field of our ENDOR system. This value, 0.196 MHz in frequency units, agrees satisfactorily with the experimentally observed splitting.

An appropriate candidate for the likewise positive coupling constant, $a_{H\beta''}$, of the second pair of β-protons in the same methylene groups is 0.059 mT, as the sum $|a_{H\beta'} + a_{H\beta''}|$ measured by ESR spectroscopy in the intermediate exchange rate amounts to 2.216 ± 0.020 mT at 298 K[4] and to 2.24 ± 0.02 mT at 243 K. These values agree, in the limits of experimental error, with the sum (2.182 ± 0.008) mT + (0.059 ± 0.002) mT = 2.241 ± 0.010 mT obtained by ENDOR spectroscopy at the slow exchange rate (193 K).

Going from $\mathbf{3}^{\bullet+}$ to $\mathbf{3}\text{-}d_2^{\bullet+}$, i.e., replacing the two methylene γ-protons by deuterons, leads to the disappearance of the ENDOR signals associated with −0.246 and −0.129 mT. Consequently, these values represent the coupling contants, $a_{H\gamma'}$ and $a_{H\gamma''}$, of two methylene γ-protons which are not equivalent at 193 K, and the remaining a_H values of −0.210, −0.203, +0.174, +0.154, and 0.009 mT observed in this temperature are left for the protons at the π-perimeter ($a_{H\mu}$).

The signals associated with the coupling constant, a_N, of the two ^{14}N nuclei, which is not affected by the conformational interconversion of the trimethylene chain, could not be detected by the ENDOR technique at 193 K, but they became evident at 243 K. Figure 2 (bottom) shows the ^{14}N and proton ENDOR spectrum at this temperature. The $|a_N|$ value derived from the ENDOR signals at the frequencies $^1/_2|a_N| \pm \nu_N$ is 1.695 ± 0.005 mT and thus agrees in the limits of experimental error with the previously reported value; the sign of a_N is certainly positive. At 243 K, only two pairs of proton ENDOR signals at $\nu_H \pm {}^1/_2|a_H|$ are observed. The coupling constants associated with them, $\bar{a}_{H\mu}$ = −0.206 ± 0.003 (4 H) and +0.165 ± 0.002 mT (4 H), represent the averages of two-proton $a_{H\mu}$ values found at 193 K, $^1/_2[-0.210 + (-0.203)]$ and $^1/_2(+0.174 + 0.154)$ mT, respectively; their opposite signs have been confirmed by TRIPLE resonance spectroscopy. The signals arising from the methylene β- and γ-protons are here broadened beyond recognition. Clearly, whereas the coupling constants of the corresponding perimeter protons (differences: $|\Delta a_{H\mu}|$ = 0.007 and 0.020 mT) are already averaged out at 243 K, this is not yet the case for the methylene protons ($|\Delta a_{H\beta}|$ = 2.123 and $|\Delta a_{H\gamma}|$ = 0.117 mT).

The trimethylenediimino[14]annulene **3**-Br, in which a Br atom occupies the 2-position of the perimeter, could also readily be oxidized to its radical cation. The ESR spectrum of $\mathbf{3}\text{-Br}^{\bullet+}$, taken at 243 K, indicates that the number of perimeter protons giving rise to hyperfine splittings of 0.16–0.21 mT (0.185 ± 0.025 mT) has decreased by 1. Thus, the proton eliminated by the bromination at the π-center μ = 2 must have a coupling constant, $|a_{H\mu}|$, of this size. It is noteworthy that the two ^{14}N atoms in $\mathbf{3}\text{-Br}^{\bullet+}$ are distinctly nonequivalent as expected for lowering the symmetry on going from $\mathbf{3}^{\bullet+}$ to $\mathbf{3}\text{-Br}^{\bullet+}$. At 243 K, the ^{14}N ENDOR spectrum of $\mathbf{3}\text{-Br}^{\bullet+}$ exhibits two pairs of signals at $^1/_2|a_N| \pm \nu_N$; they are associated with the coupling constants a_N = +1.66 ± 0.01 and +1.73 ± 0.01 mT.

***N,N'*-Tetramethylene-*syn*-1,6:8,13-diimino[14]annulene (4).** ESR spectra of $\mathbf{4}^{\bullet+}$ at 193, 228, and 273 K were shown in a previous communication.[5] Their pronounced temperature dependence is due to the conformational interconversion of the tetramethylene chain (activation energy 22 ± 2 kJ/mol).[5] In contrast to $\mathbf{3}^{\bullet+}$, no ESR spectra characteristic of a slow exchange rate have been observed, because they require temperatures below the freezing point (178 K) of the solvent (dichloromethane). The range of the intermediate exchange rate extends up to 273 K, at which temperature an averaged value, $\bar{a}_{H\beta}$, is apparent for the two pairs of methylene β-protons. This value has been reported[5] as +0.72 ± 0.01 mT (4 H), along with the ^{14}N coupling constant, a_N = +2.57 ± 0.01 mT (2 N), which is not affected by the conformational changes (the sign of both $\bar{a}_{H\beta}$ and a_N is certainly positive).

An ENDOR spectrum taken in the present work at 193 K, i.e., in the range of an intermediate exchange rate, reveals only the presence of the perimeter protons, with the signals from the β- and γ-methylene protons being broadened beyond recognition. The coupling constants, −0.188 ± 0.002 (4 H), −0.154 ± 0.002 (4 H), and 0.012 ± 0.001 mT (2 H, sign undetermined), represent the averaged values $\bar{a}_{H\mu}$.[12] On raising the temperature to 243 K, ENDOR signals of γ-methylene protons can also be observed, the averaged coupling constant $\bar{a}_{H\gamma}$ being −0.051 ± 0.001 mT (4 H). The sign of these $a_{H\mu}$ values has been determined by a general TRIPLE resonance experiment and by analogy with the corresponding data for $\mathbf{1}^{\bullet+}$–$\mathbf{3}^{\bullet+}$. The assignment of −0.051 mT to the γ-protons has been confirmed by the ENDOR spectrum of $\mathbf{4}\text{-}d_4^{\bullet+}$ at 243 K, as the signals associated with this coupling constant are eliminated on replacing the four γ-protons in $\mathbf{4}^{\bullet+}$ by deuterons.

A ^{14}N ENDOR signal is likewise detected at 243 K. It is positioned at $^1/_2|a_N| - \nu_N$, while its counterpart at $^1/_2|a_N| + \nu_N$ is outside the frequency range (35 MHz) available to our ENDOR system. The coupling constant a_N associated with this signal agrees in the limits of experimental error with the value derived previously from the ESR spectra.[5] Upon a further rise of the temperature to 273 K, ENDOR signals associated with the averaged coupling constant, $\bar{a}_{H\beta}$, of the four methylene β-protons become discernible. The $\bar{a}_{H\beta}$ value determined from the positions, $\nu_H \pm {}^1/_2|a_H|$, of these signals is +0.718 ± 0.005 mT, in agreement with that reported in the previous communication.[5]

The resolution of the ESR spectra of $\mathbf{4}^{\bullet+}$ and $\mathbf{4}\text{-}d_4^{\bullet+}$ is greatly improved at higher temperatures. This is illustrated in Figure 3 by a spectrum of $\mathbf{4}\text{-}d_4^{\bullet+}$ taken at 313 K.

***N,N'*-Penta-, *N,N'*-Hexa-, and *N,N'*-Heptamethylene-*syn*-1,6:8,13-diimino[14]annulenes (5–7).** Lengthening of the conformationally flexible polymethylene chain makes the ESR spectra of the radical cations $\mathbf{5}^{\bullet+}$, $\mathbf{6}^{\bullet+}$, and $\mathbf{7}^{\bullet+}$ increasingly more complicated due to their temperature dependence. Analyses of these spectra could be carried out with the use of the ENDOR technique, but the resulting proton hyperfine data do not provide additional information relevant to the subsequent discussion. Therefore, in order to avoid undue expansion of the paper, these data are not considered here. On the other hand, it is advisable to quote the ^{14}N coupling constants which do not markedly depend on the temperature and which are highly informative with respect to the structure of the radical cations. The a_N values (in millitesla) are as follows: +2.72 ± 0.01 (2 N), +2.57 ± 0.01 (2 N), and +2.62 ± 0.01 (2 N) for $\mathbf{5}^{\bullet+}$, $\mathbf{6}^{\bullet+}$, and $\mathbf{7}^{\bullet+}$, respectively.

***N,N'*-Dimethyl-*syn*-1,6:8,13-diimino[14]annulene (8).** Due to the replacement of the polymethylene chain linking the two N atoms by two freely rotating methyl groups, the ESR spectra of $\mathbf{8}^{\bullet+}$ are largely temperature independent. Figure 4 shows a spectrum taken at 298 K. Its prominent features are the total width of 19 mT, quite unusual for an organic radical ion, and the apparent asymmetry is caused by second-order effects. The undoubtedly positive coupling constants of the two ^{14}N nuclei and the six methyl β-protons, a_N and $a_{H\beta}$, are as follows (in millitesla): +2.66 ± 0.01 (2 N) and +1.213 ± 0.005 (6 H). The a_N value gives rise to a second-order splitting of $(a_N)^2/2B_0$ = 0.010 mT that is large enough to affect the ESR spectrum. Additional coupling constants determined by the ENDOR technique are those of the perimeter protons: $a_{H\mu}$ = −0.189 ± 0.002 (4 H) and +0.172

(11) Evans, J. C.; Obaid, A. Y.; Rowlands, C. C. *Chem. Phys. Lett.* **1984**, *109*, 398.

(12) These values are more accurate than those given previously.[5]

Table II. ^{14}N and Proton Coupling Constants, a_N and a_H, for $1^{\bullet+}$, 1-$Me_2^{\bullet+}$, $2^{\bullet+}$–$4^{\bullet+}$, and $8^{\bullet+}$ [a]

radical cation	temp, K	a_N, mT	$a_{H\beta}$, mT	$a_{H\gamma}$, mT	$a_{H\mu}$, mT		
					μ = 2,5,9,12	μ = 3,4,10,11	μ = 7,14
$1^{\bullet+}$	233	+0.633 (2N)	<0.01 (2H)		+0.062 (4H)	−0.143 (4H)	<0.01 (2H)
1-$Me_2^{\bullet+}$	243	+0.714 (2N)		<0.01 (6H)	+0.106 (4H)	−0.128 (4H)	0.014 (2H)[b]
$2^{\bullet+}$	193	+0.611 (2N)	+0.090 (4H)		+0.076 (4H)	−0.145 (4H)	<0.01 (1H)
$3^{\bullet+}$	193	+1.70 (2N)	+2.182 (2H)	−0.246 (1H)	+0.174 (2H)	−0.210 (2H)	0.009 (1H)[b]
			+0.059 (2H)	−0.129 (1H)	+0.154 (2H)	−0.203 (2H)	<0.005 (1H)
	243	+1.69 (2N)	+1.12 (4H)[c,d]	−0.185 (2H)[c,e]	+0.165 (4H)[c]	−0.206 (4H)[c]	<0.01 (2H)
$4^{\bullet+}$	273	+2.57 (2N)	+0.718 (4H)[c]	−0.051 (4H)[c]	+0.154 (4H)[c]	−0.188 (4H)[c]	0.012 (2H)[b,c]
$8^{\bullet+}$	298	+2.66 (2N)	+1.213 (6H)		+0.172 (4H)	−0.189 (4H)	<0.02 (2H)

[a] Experimental error indicated in text. [b] Sign undetermined. [c] Averaged values. [d] Half the value $|a_{H\beta'} + a_{H\beta''}|$ = 2.24 mT. [e] Observed at temperatures above 270 K.

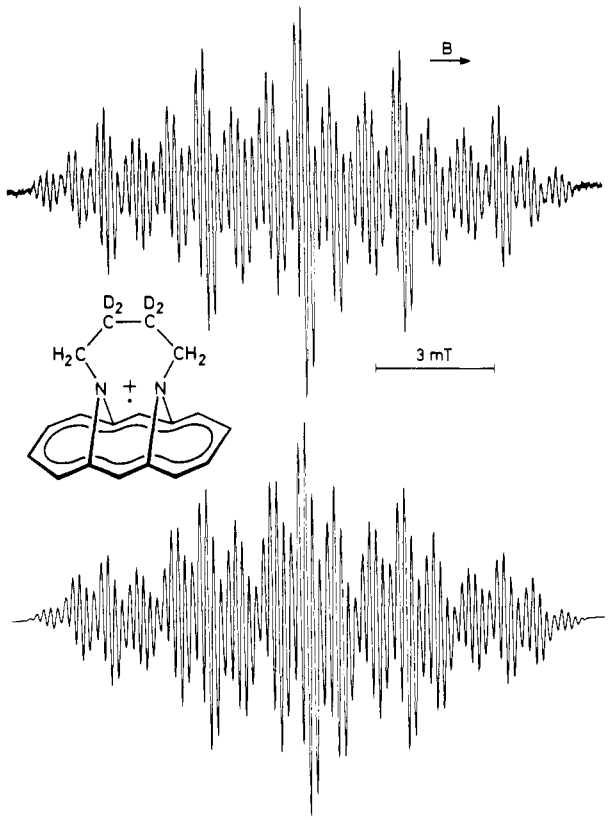

Figure 3. ESR spectrum of **4**-$d_4^{\bullet+}$ (top) and its simulation (bottom): solvent, CH_2Cl_2; counterion, $SbCl_6^-$; temperature, 313 K. The simulation makes use of the ^{14}N and proton coupling constants given for $4^{\bullet+}$ in the text and Table II, with the $|a_{H\gamma}|$ value of 0.051 mT being replaced by $|a_{D\gamma}|$ = 0.008 mT (both unresolved); line shape Lorentzian, line width 0.12 mT.

± 0.002 mT (4 H). Their signs are indicated by the TRIPLE resonance experiment and by comparison with the corresponding values for other radical cations in this series.

Table II summarizes the ^{14}N and proton coupling constants, a_N and a_H, for $1^{\bullet+}$, 1-$Me_2^{\bullet+}$, $2^{\bullet+}$, $3^{\bullet+}$, $4^{\bullet+}$, and $8^{\bullet+}$. Assignments of the $a_{H\mu}$ values to sets of equivalent protons at the perimeter π-centers μ have been based on theoretical arguments presented in the Discussion. The g factors of $1^{\bullet+}$, 1-$Me_2^{\bullet+}$, and $2^{\bullet+}$ are 2.0029, 2.0031, and 2.0033, respectively; those of $3^{\bullet+}$–$8^{\bullet+}$ are all 2.0036 within the experimental error of ±0.0001.

Discussion

Electronic Structure. In Figure 5, the total widths of the ESR spectra are compared for the radical anions[13] and for the corresponding radical cations (this work) of the diimino[14]annulenes **1**, 1-Me_2, and **2**–**8**. Such a comparison provides a convenient starting point for the discussion of the electronic structure of $1^{\bullet+}$–$8^{\bullet+}$.

(13) Gerson, F.; Knöbel, J.; Lopez, J.; Vogel, E. *Helv. Chim. Acta* **1985**, *68*, 371. Gerson, F.; Gescheidt, G.; Vogel, E. Unpublished data.

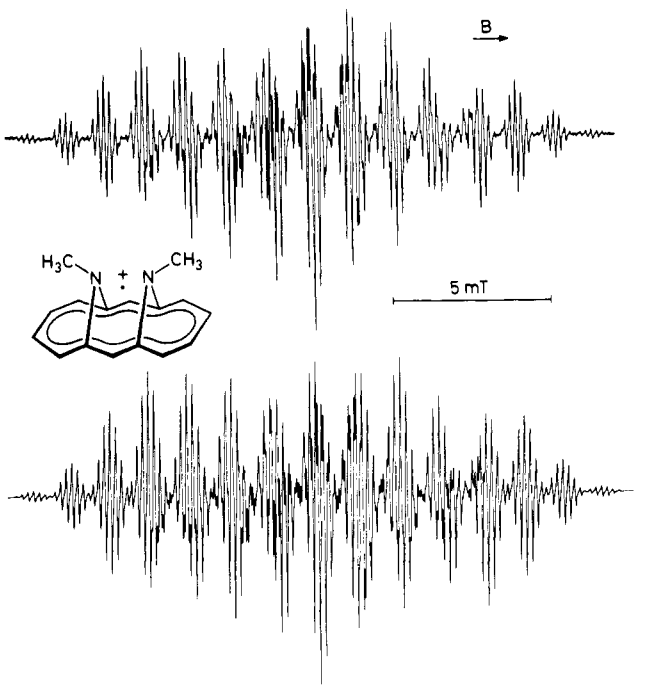

Figure 4. ESR spectrum of $8^{\bullet+}$ (top) and its simulation (bottom): solvent, CH_2Cl_2; counterion, $SbCl_6^-$; temperature, 298 K. The simulation makes use of the ^{14}N and proton coupling constants given in the text and Table II, and it accounts for the second-order splittings; line shape Lorentzian, line width 0.04 mT.

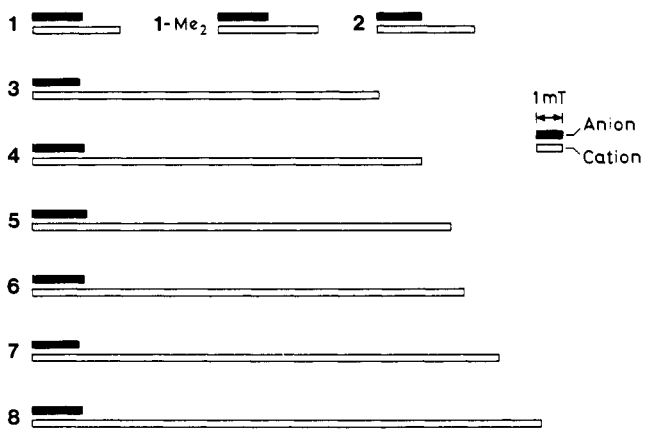

Figure 5. Schematic presentation of the total widths of the ESR spectra observed for the radical anions and the radical cations of **1**, 1-Me_2, and **2**–**8**.

For the radical anions, the total widths of the spectra are relatively small and of similar magnitudes, 1.7–2.1 mT, throughout the whole series. On going to the corresponding radical cations, there is a remarkable increase in these widths. Moreover, such an increase differs for the individual diimines, the total widths being 3.3–3.8 mT for $1^{\bullet+}$, 1-$Me_2^{\bullet+}$, and $2^{\bullet+}$ but 13–19 mT for

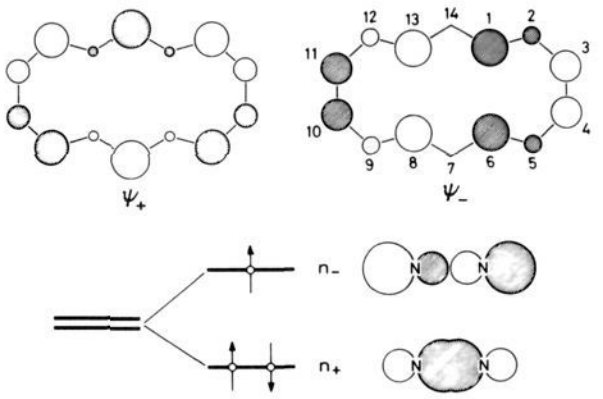

Figure 6. Diagrams of the perimeter HOMOs, ψ_+ and ψ_-, and the N lone pairs MO's n_+ and n_-. Occupancy of n_+ and n_- in $\mathbf{1}^{\bullet+}$–$\mathbf{8}^{\bullet+}$.

$\mathbf{3}^{\bullet+}$–$\mathbf{8}^{\bullet+}$. One notes that the former three radical cations have been classified as L and the six latter ones as M, according to their thermodynamic and kinetic stabilities (see Results).

The differences in the total widths can be interpreted as follows. The unpaired electron in the radical anions occupies a nearly "pure" π-perimeter HOMO ψ_+, which is symmetric with respect to the vertical plane passing through the centers 7 and 14 in **1**–**8** (Figure 6). The spin population is almost exclusively confined to the 14-membered perimeter, with only marginal delocalization onto the imino bridging groups.[13] By contrast, the unpaired electron in the radical cations is predominantly located in an orbital n_- representing an antibonding combination of the N lone pairs. The single occupancy of n_- is in accord with the vanishingly small coupling constants, $a_{H\beta}$ and $a_{H\gamma}$, of the methylene and methyl protons in $\mathbf{1}^{\bullet+}$ and **1**-$Me_2^{\bullet+}$ (Table II), which are situated in the nodal plane of this orbital. The "natural" sequence, n_- *above* n_+ (Figure 6), indicates a predominant through-space interaction between the N lone pairs.[14] The orbital n_- can combine with the perimeter HOMO ψ_-, which is antisymmetric with respect to the vertical plane through the centers 7 and 14. The bulk of the spin population is thus accommodated in the orbital n_- at the N atoms with some delocalization onto the perimeter HOMO ψ_-. In other words, $\mathbf{1}^{\bullet-}$, **1**-$Me_2^{\bullet-}$, and $\mathbf{2}^{\bullet-}$–$\mathbf{8}^{\bullet-}$ are *cyclic* π*-radicals*, whereas their positively charged counterparts $\mathbf{1}^{\bullet+}$, **1**-$Me_2^{\bullet+}$, and $\mathbf{2}^{\bullet+}$–$\mathbf{8}^{\bullet+}$ have to be considered as *N-centered radicals*.

Inspection of the hyperfine data for the radical cations in Table II indicates that the coupling constants, $a_{H\mu}$, of the perimeter protons are relatively small and not greatly different within classes L and M. The two four-proton sets having the $a_{H\mu}$ values of −0.13 to −0.21 mT and +0.06 to +0.18 mT have tentatively been identified with those at the centers μ = 3, 4, 10, 11 and 2, 5, 9, 12, respectively, as such an assignment is clearly more compatible with the LCAO coefficients for ψ_- than the reverse one (Figure 6). The two remaining perimeter protons at the centers μ = 7, 14, i.e., in the nodal plane of ψ_-, have vanishingly small coupling constants which are only occasionally observable (Table II).

The strikingly enlarged total widths of the ESR spectra for the radical cations of class M ($\mathbf{3}^{\bullet+}$–$\mathbf{8}^{\bullet+}$) relative to those of class L ($\mathbf{1}^{\bullet+}$, **1**-$Me_2^{\bullet+}$, and $\mathbf{2}^{\bullet+}$) can be traced back to the differing ^{14}N and β-proton coupling constants, a_N and $a_{H\beta}$. In Figure 7, the a_N values, determined by ESR and ENDOR spectroscopy for $\mathbf{1}^{\bullet+}$–$\mathbf{8}^{\bullet+}$, are correlated with the arrangement of the C–N bonds about the N atoms, as deduced from the X-ray crystallographic data of **1**,[2b] **2**,[2b] $\mathbf{3}^{2b}/\mathbf{3}^{\bullet+}$,[4] $\mathbf{4}^{5}/\mathbf{4}^{\bullet+}$,[5] **6**,[2c] **7**,[2c] and **8**[1b] and from molecular models of **5**. The structural features underlying the classification of the radical cations into L and M are now obvious. In those of class L ($\mathbf{1}^{\bullet+}$ and $\mathbf{2}^{\bullet+}$, as well as **1**-$Me_2^{\bullet+}$), the small size of the groups linking the N atoms forces the lone pairs to be directed "outward". Consequently, the interaction of these pairs is slight and so is their energetic splitting into n_+ and n_-. As the destabilizing contribution of the unpaired electron in n_- is hardly outweighed by the stabilization due to the two paired electrons in n_+, the thermodynamic and kinetic stabilities are low. Moreover, the "outer" orientation of the N lone pairs does not favor the formation of an N–N three-electron σ-bond, and the ^{14}N coupling constants, a_N, have only a moderate size (0.6–0.7 mT). By contrast, in the radical cations of class M, a longer polymethylene chain ($\mathbf{3}^{\bullet+}$–$\mathbf{7}^{\bullet+}$) or *N*-methyl substituents ($\mathbf{8}^{\bullet+}$) allow the lone pairs to be directed "inward". The strong interaction of these pairs leads to a large energy gap between n_- and n_+, so that the destabilizing contribution of the unpaired electron in n_- is greatly overcompensated by the stabilization due to the paired electrons in n_+; this interaction results in high thermodynamic and kinetic stabilities. The "inward" orientation favors formation of an N–N three-electron σ-bond and the ^{14}N coupling constants, a_N, are large (1.7–2.7 mT).

The occurrence of such an N–N σ-bond in the radical cations of class M has been, in two cases, directly confirmed by X-ray crystallographic structure analyses. Thus, on passing from **3** to $\mathbf{3}^{\bullet+}$ and from **4** to $\mathbf{4}^{\bullet+}$, the interatomic N–N distance is reduced from 270.5[2b] to 216.0 pm[4] and from 256.0[5] to 218.9 pm,[5] respectively. Furthermore, with the use of the ESR and X-ray data for $\mathbf{3}^{\bullet+}$, $\mathbf{4}^{\bullet+}$, and the radical cation of 1,6-diazabicyclo[4.4.4]-tetradecane (**9**),[3c] a nearly perfect linear relation $a_N = (46.18 \pm 0.30) - (0.3736 \pm 0.0026)\chi$ has been established between the ^{14}N coupling constants (a_N in millitesla) and the average C–N–C angle (χ in degrees).[5] An increase in the a_N value from 1.69 ($\mathbf{3}^{\bullet+}$) to 2.57 ($\mathbf{4}^{\bullet+}$) to 3.59 mT ($\mathbf{9}^{\bullet+}$) goes along with a decrease in the angle χ from 119.1 to 116.7 to 114.0°, respectively. These changes reflect a growing s-contribution to the "character" of the N–N three-electron σ-bond. In $\mathbf{3}^{\bullet+}$ (χ = 119.1°), this bond has almost "pure" p-character (Figure 7), being nearly perpendicular to the plane of the two "flat" N atoms which are thus approximately sp^2-hybridized. In $\mathbf{4}^{\bullet+}$ (χ = 116.7°), their hybridization changes from sp^2 in the direction of sp^3, and each increasingly deviates from the coplanar arrangement with three neighboring C atoms. Although no X-ray data are available for $\mathbf{5}^{\bullet+}$, $\mathbf{6}^{\bullet+}$, and $\mathbf{7}^{\bullet+}$, the geometry about the N atoms must be similar to that in $\mathbf{4}^{\bullet+}$ (Figure 7). This statement is consistent with the a_N values which are not greatly altered upon further elongation of the polymethylene chain. In fact, the ^{14}N coupling constants for $\mathbf{4}^{\bullet+}$–$\mathbf{7}^{\bullet+}$ only oscillate slightly about 2.66 mT, an a_N value found for the *N,N'*-dimethyl-substituted radical cation $\mathbf{8}^{\bullet+}$ that may be considered to have its two N atoms linked by an infinitely long polymethylene chain.

Interpretation of the relatively low a_N values (0.6–0.7 mT) for the radical cations of class L is more problematic. Evidently, the linear relation between a_N and χ found for the radical cations with the inward-directed N lone pairs does not apply to $\mathbf{1}^{\bullet+}$, **1**-$Me_2^{\bullet+}$, and $\mathbf{2}^{\bullet+}$, in which these pairs are oriented outward.

To gain more insight into the N···N interaction, INDO calculations[15] were performed on two simple models of the relevant diimino fragments of the radical cations $\mathbf{1}^{\bullet+}$–$\mathbf{4}^{\bullet+}$. Both models are related to the X-ray crystallographic structures of **1**,[2b] **2**,[2b] $\mathbf{3}^{\bullet+}$,[4] and $\mathbf{4}^{\bullet+}$.[5] Geometries of the neutral molecules **1** and **2** had to be used for lack of the X-ray data of $\mathbf{1}^{\bullet+}$ and $\mathbf{2}^{\bullet+}$, which did not yield stable crystalline salts. However, the structures of these two radical cations should not markedly deviate from those of the neutral molecules, as no N–N three-electron bond is formed and as the CH_2 and the CH_2CH_2 bridges are rather rigid.

The first model involves the radical cation $[H_3N\cdots NH_3]^{\bullet+}$, which has previously been subjected to ab initio calculations.[7] The six C atoms of the imino fragments were replaced by H atoms, and the N–H bond lengths were fixed at 100 pm. The N···N distances as well as the bond and dihedral angles were taken from the crystallographic data of **1**, **2**, $\mathbf{3}^{\bullet+}$, and $\mathbf{4}^{\bullet+}$ (Figure 8). Whereas the experimental ^{14}N coupling constants, a_N, for $\mathbf{3}^{\bullet+}$ and $\mathbf{4}^{\bullet+}$ correlate very well with the calculated data, the agreement is fair for $\mathbf{2}^{\bullet+}$ and a high discrepancy exists for $\mathbf{1}^{\bullet+}$ (Table III). It arises

(14) Hoffmann, R.; Imamura, A.; Hehre, W. J. *J. Am. Chem. Soc.* **1968**, *90*, 1499. Hoffmann, R. *Acc. Chem. Res.* **1971**, *4*, 1.

(15) Pople, J. A.; Beveridge, D. L. *Approximate Molecular Orbital Theory*; McGraw-Hill: New York, 1970.

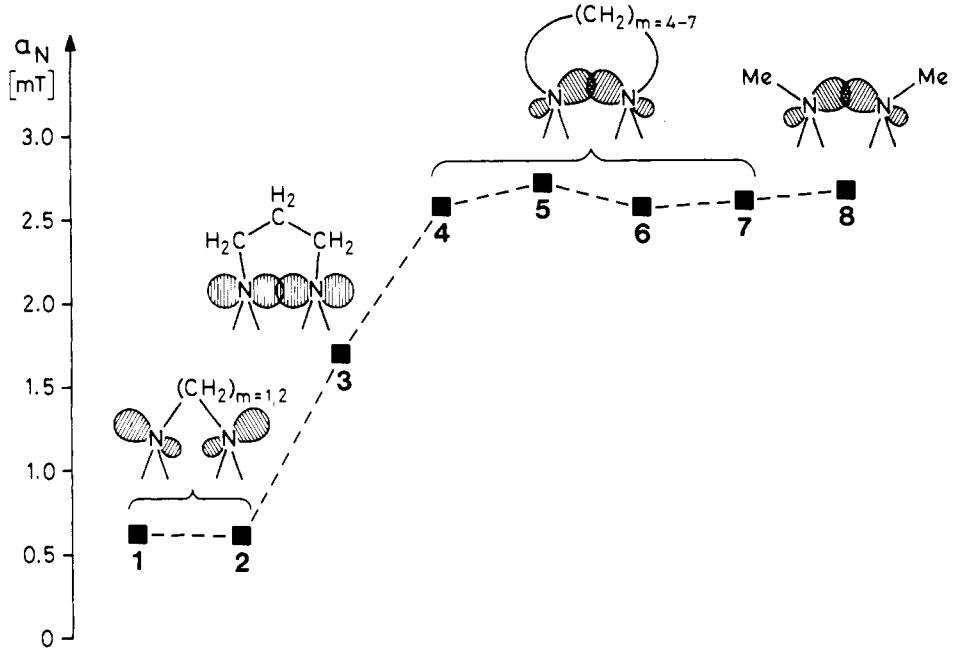

Figure 7. Correlation of the ^{14}N coupling constants, a_N, with the geometry about the N atoms in **1–8**.

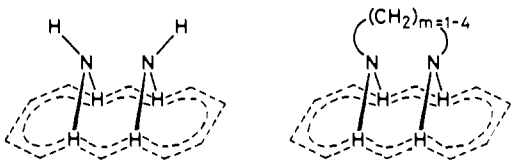

Figure 8. Models $[H_3N\cdots NH_3]^{\bullet+}$ (left) and $[H_2N-(CH_2)_m-NH_2]^{\bullet+}$ (right) of $\mathbf{1}^{\bullet+}$–$\mathbf{4}^{\bullet+}$.

Table III. Calculated vs Observed ^{14}N Coupling Constants, a_N (in mT), for $\mathbf{1}^{\bullet+}$–$\mathbf{4}^{\bullet+}$

radical cation	model $[H_3N\cdots NH_3]^{\bullet+}$	model $[H_2N-(CH_2)_m-NH_2]^{\bullet+}$	experiment
$\mathbf{1}^{\bullet+}$	−0.32,[a] +0.65[b]	+0.32	+0.63
$\mathbf{2}^{\bullet+}$	+0.96	+1.28	+0.61
$\mathbf{3}^{\bullet+}$	+1.67	+1.82	+1.69
$\mathbf{4}^{\bullet+}$	+2.45	+2.35	+2.57

[a] N···N distance, 243 pm. [b] N···N distance, 280 pm; cf. text.

from replacing the CH_2 group in $\mathbf{1}^{\bullet+}$ by two H atoms while preserving the short interatomic distance of 243 pm. As a consequence, the two H atoms are forced into closer contact than allowed by their van der Waals radii, thus yielding nonrealistic spin densities at the N atoms. When the N···N distance is increased to 280 pm in order to avoid the interference of the H atoms, the calculated a_N value gets closer to its experimental counterpart.

In the second model, represented by $[H_2N(CH_2)_mNH_2]^{\bullet+}$, the four N–C links to the π-perimeter were again replaced by N–H (length 100 pm), but the polymethylene chain between the N atoms was incorporated (Figure 8). Again, the observed ^{14}N coupling constants for $\mathbf{3}^{\bullet+}$ and $\mathbf{4}^{\bullet+}$ are in good agreement with the corresponding INDO-calculated a_N values, while those for $\mathbf{1}^{\bullet+}$ and $\mathbf{2}^{\bullet+}$ exhibit differences between theory and experiment (Table III). In this model the discrepancy is particularly large for $\mathbf{2}^{\bullet+}$ because of the reversal in the "natural" sequence of n_+ and n_- orbitals by the INDO calculations. Such a reversal, which places n_+ *above* n_-, results from a through-space interaction being overruled by a through-bond mechanism; in $\mathbf{2}^{\bullet+}$, the latter is favored by the presence of the CH_2CH_2 bridging group.[14,16] As a consequence, the INDO calculation requires that the singly occupied orbital in $\mathbf{2}^{\bullet+}$ should be represented by n_+ and not by

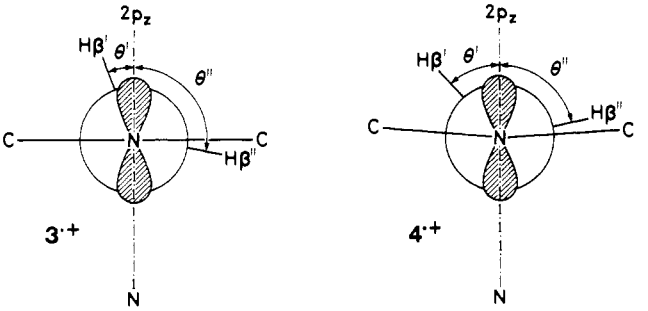

Figure 9. Newman projections illustrating the conformation of the polymethylene chains in $\mathbf{3}^{\bullet+}$ and $\mathbf{4}^{\bullet+}$.

n_- as in $\mathbf{1}^{\bullet+}$, $\mathbf{3}^{\bullet+}$, and $\mathbf{4}^{\bullet+}$, thus leading to a much too high a_N value. However, the proton coupling constants, $a_{H\mu}$, observed for $\mathbf{2}^{\bullet+}$ (Table II) do not indicate a change in the symmetry of the singly occupied orbital in $\mathbf{2}^{\bullet+}$ relative to $\mathbf{1}^{\bullet+}$, $\mathbf{3}^{\bullet+}$, and $\mathbf{4}^{\bullet+}$, so that the INDO energy sequence and the a_N value seem to be at variance with experiment.

Despite the above-stated shortcomings for $\mathbf{1}^{\bullet+}$ and $\mathbf{2}^{\bullet+}$, the general trend of increasing a_N values with the lengthening of the polymethylene chain in the series $\mathbf{1}^{\bullet+}$–$\mathbf{4}^{\bullet+}$ is reproduced by the calculations. In particular, it is gratifying to note that the substantially lower values for $\mathbf{1}^{\bullet+}$ and $\mathbf{2}^{\bullet+}$ than for $\mathbf{3}^{\bullet+}$ and $\mathbf{4}^{\bullet+}$ are accounted for. A more quantitative agreement between theory and experiment can, in general, hardly be expected with the use of oversimplified models for large radical cations.

Conformation of the Polymethylene Chains. The coupling constants, $a_{H\beta}$, of the methylene β-protons in $\mathbf{4}^{\bullet+}$–$\mathbf{7}^{\bullet+}$ are less informative than their ^{14}N counterparts a_N with respect to the electronic structure and geometry of the N atoms, because they depend strongly on the conformation of the polymethylene chains. Using the relation[17] $a_{H\beta} = B\rho_N \cos^2\theta$, where B, ρ_N, and θ are a proportionality factor, the $2p_z$ spin population at the adjacent N atom, and the dihedral angle between the C–Hβ and the axis of the N $2p_z$ AO, respectively, one can get information about the preferred conformation of this chain. For $\mathbf{3}^{\bullet+}$, the observed values $a_{H\beta'} = +2.182$ and $a_{H\beta''} = +0.059$ mT are consistent with the dihedral angles $\theta' = 21°$ and $\theta'' = 99°$ and $B\rho_N = +2.51$ mT (θ' and θ'' should add to 120°; Figure 9). A similar value of $B\rho_N$

(16) Heilbronner, E.; Muszkat, K. A. *J. Am. Chem. Soc.* **1970**, *92*, 3818.

(17) Heller, C.; McConnell, H. M. *J. Chem. Phys.* **1960**, *32*, 1535. Horsfield, A.; Morton, J. R.; Whiffen, D. H. *Mol. Phys.* **1961**, *4*, 425.

= +2.43 mT is obtained from $a_{H\beta}$ = +1.213 mT for $8^{\bullet+}$, as $\cos^2\theta = 0.5$ for freely rotating methyl groups. Obviously, the large increase in the ^{14}N coupling constant, a_N, on going from $3^{\bullet+}$ to $4^{\bullet+}$–$8^{\bullet+}$ requires only a slight enhancement in the s-character of the N–N three-electron σ-bond and does not greatly affect the $2p_z$ spin population ρ_N. For $4^{\bullet+}$, the $B\rho_N$ value of +2.43 mT and the averaged β-proton coupling constant $\bar{a}_{H\beta}$ = +0.718 mT can be used to estimate the dihedral angles θ' and θ'', even in the absence of experimental data for $a_{H\beta'}$ and $a_{H\beta''}$. The angles θ' and θ'' thus obtained are 42° and 78° (Figure 9).

Conclusions

The cations of the *N,N'*-polymethylene-*syn*-1,6:8,13-diimino-[14]annulenes **1**–**7** have to be regarded as N-centered radicals, in which the two N atoms bear the bulk of the spin population. The singly occupied orbital is predominantly the antibonding combination, n_-, of the N lone pairs, as required by an interaction of the through-space type. The s-character of this orbital at the N atoms, and therewith the size of the ^{14}N coupling constant, a_N, is a function of the local geometry of the diimino fragment which, in turn, critically depends on the length of the $(CH_2)_m$ chain. For m = 1 or 2, as in **1** and **2**, the relatively weak interaction between the outward-directed lone pairs reduces the a_N value (0.6–0.7 mT). On the other hand, when $m \geq 3$, as in **3**–**7**, the interaction between inward-oriented lone pairs enhances this value (1.7–2.7 mT); an N–N three-electron σ-bond is formed upon oxidation of these compounds to their radical cations. Formation of such a bond is also indicated for the *N,N'*-dimethyl derivative **8** on its conversion to $8^{\bullet+}$, whereby this diimine may be considered as having a very long polymethylene chain. It is undoubtedly this N–N σ-bond which bestows unusual kinetic and thermodynamic stabilities on the radical cations $3^{\bullet+}$–$8^{\bullet+}$.

Experimental Section

Solvents and Reagents. The solvents were dried by standard procedures and distilled before use. Merck alumina (Brockmann, basic, act. II–III) and Merck silica gel (mesh 70–230) were employed in column chromatography. The reagents used for the oxidation were commercial chemicals (FLUKA or Merck), with the exception of tris(*p*-bromophenyl)ammoniumyl hexachloroantimonate which was prepared according to a known procedure.[18]

Instruments and Measurements. The ^1H and ^{13}C NMR spectra of the compounds were recorded at 300 and 75.5 MHz, respectively, on a Bruker AM 300 spectrometer; the chemical shifts are reported relative to tetramethylsilane. Mass spectra were obtained on a MAT212 or a Finnigan 3200 spectrometer. IR spectra were measured on a Perkin-Elmer 283 infrared spectrophotometer. Elemental analyses were performed by Bayer AG, Leverkusen. Melting points are uncorrected. The cyclic voltammograms were recorded on a potentiostat 173/universal programmer 175 of Princeton Applied Research (PAR) or on a Metrohm-Polarecord E 56/VA Scanner 612/VA Stand 663. The ESR spectra were taken on a Varian-E9 instrument, while a Bruker-ESP-300 system served for ENDOR and TRIPLE resonance studies.

Preparation of Compounds. The compounds **1**–**8** and their derivatives were prepared from *syn*-1,6:8,13-diimino[14]annulene according to Scheme I. The synthesis of the parent diimine was described several years ago,[1a] and that of **3**[4] and **4**[5] was outlined in previous communications.

***N,N'*-Methylene-*syn*-1,6:8,13-diimino[14]annulene (1).** A solution of *syn*-1,6:8,13-diimino[14]annulene (312 mg, 1.5 mmol) in dichloromethane (50 mL) was shaken vigorously with aqueous formaldehyde (40%, 15 mL) for 1 min. The mixture was washed with water, and the organic phase was dried over magnesium sulfate. Chromatography with ether on alumina (10 × 1.5 cm) and crystallization from ether yielded **1** (312 mg, 94%) as blue-black needles (mp = 184–185 °C): ^1H NMR (CD_2Cl_2) δ 8.54 (s, 2 H), 7.76–7.68 and 7.52–7.44 (AA'BB' system, 8 H), 1.21 (s, 2 H); ^{13}C NMR (CD_2Cl_2) δ 129.38, 123.79, 123.37, 116.60, 58.99; MS (70 eV) *m/e* 220 (100) M^+, 191 (26) $[M - CH_3N]^+$; IR (CsI) 3035, 1530 cm^{-1}; UV–vis (MeOH) λ_{max}, nm (ϵ) 282 (57 500), 346 (42 000), 405 sh (7500), 581 (1500). Anal. Calcd for $C_{15}H_{12}N_2$: C, 81.79; H, 5.49; N, 12.73. Found: C, 81.6; H, 5.5; N, 12.8.

***N,N'*-Perdeuteriomethylene-*syn*-1,6:8,13-diimino[14]annulene (1-d_2)** was prepared from the parent diimine and formaldehyde-d_2 (Rohstoff Einfuhr GmbH, Düsseldorf) by the same procedure as that for the unlabeled compound **1**.

Scheme I

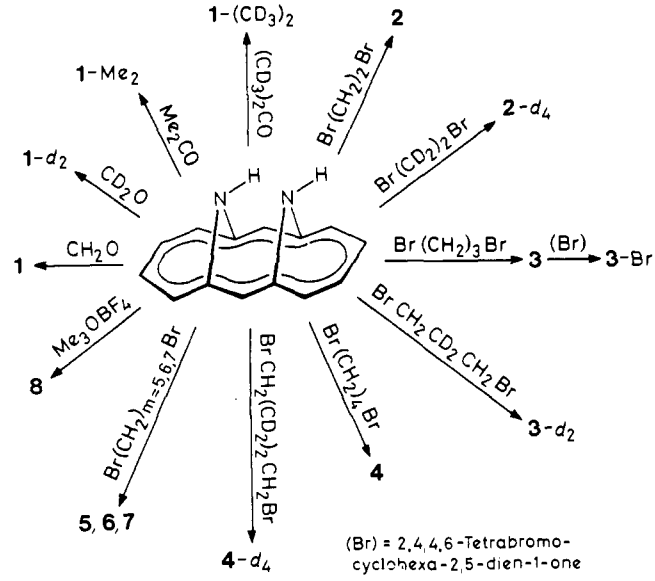

***N,N'*-Isopropylidene-*syn*-1,6:8,13-diimino[14]annulene (1-Me_2).** *syn*-1,6:8,13-Diimino[14]annulene (312 mg, 1.5 mmol) was refluxed in acetone (100 mL) for 4 h. After evaporation of the solvent, the crude product was chromatographed with ether on silica gel (10 × 1.5 cm). Crystallization from ethyl acetate/pentane (1:1) yielded **1**-Me_2 (258 mg, 69%) as red-violet needles (mp = 238–239 °C): ^1H NMR ($CDCl_3$) δ 8.50 (s, 2 H), 7.79–7.72 and 7.58–7.50 (AA'BB' system, 8 H), 0.24 (s, 6 H); ^{13}C NMR ($CDCl_3$) δ 128.95, 124.86, 124.45, 116.28, 62.07, 22.81; MS (70 eV) *m/e* 248 (100) M^+, 233 (38) $[M - CH_3]^+$, 206 (22) $[M - C_3H_6]^+$, 191 (72) $[M - C_3H_7N]^+$; IR (CsI) 3015, 1582, 1532 cm^{-1}; UV–vis (MeOH) λ_{max}, nm (ϵ) 279 (72 200), 332 (31 500), 387 sh (7800), 545 (1000).

***N,N'*-Perdeuterioisopropylidene-*syn*-1,6:8,13-diimino[14]annulene (1-$(CD_3)_2$)** was synthesized from the parent diimine and acetone-d_6 (FLUKA) by the same procedure as that for the unlabeled compound **1**-Me_2.

***N,N'*-Polymethylene-*syn*-1,6:8,13-diimino[14]annulenes (2–7): General Procedure.** A solution of *syn*-1,6:8,13-diimino[14]annulene (312 mg, 1.5 mmol), diisopropylethylamine (0.52 mL, 3 mmol), and the respective α,ω-dibromoalkane (1.5 mmol) in toluene (30 mL) was heated to 150 °C for 48 h in a sealed glass tube. The tube was rinsed with ether, and the combined organic phase was washed with water and then dried. After evaporation of the solvent, the crude product was chromatographed on alumina and crystallized from ether. The dibromoalkanes, i.e., 1,2-dibromoethane, 1,3-dibromopropane, 1,4-dibromobutane, 1,5-dibromopentane, 1,6-dibromohexane, and 1,7-dibromoheptane were commercial chemicals (FLUKA). Detailed information on the individual compounds **2**–**7** is given below.

***N,N'*-Dimethylene-*syn*-1,6:8,13-diimino[14]annulene (2)**: 135 mg (yield 39%) of red-violet prisms: mp 182–183 °C; ^1H NMR (CD_2Cl_2) δ 8.73 (s, 2 H), 7.75–7.68 and 7.49–7.42 (AA'BB' system, 8 H), 1.39 (s, 4 H); ^{13}C NMR (CD_2Cl_2) δ 134.41, 132.15, 128.92, 119.58, 48.34; MS (70 eV) *m/e* 234 (100) M^+, 206 (36) $[M - C_2H_4]^+$, 204 (43) $[M - CH_4N]^+$, 178 (79) $[M - C_2H_4N_2]^+$; IR (CsI) 3041, 2939, 2916, 1562, 1521 cm^{-1}; UV–vis (MeOH) λ_{max}, nm (ϵ) 289 (53 500), 330 (32 000), 400 sh (7500), 555 (500). Anal. Calcd for $C_{16}H_{14}N_2$: C, 82.02; H, 6.02; N, 11.96. Found: C, 82.1; H, 6.1; N, 11.8.

***N,N'*-Trimethylene-*syn*-1,6:8,13-diimino[14]annulene (3)**: 164 mg (yield 44%) of red-brown prisms: mp 154–155 °C; ^1H NMR (CD_2Cl_2) δ 9.08 (s, 2 H), 7.78–7.71 and 7.44–7.37 (AA'BB' system, 8 H), 1.23 (t, 4 H), 0.18 (q, 2 H); ^{13}C NMR (CD_2Cl_2) δ 140.93, 133.48, 128.95, 118.86, 50.29, 22.67; MS (70 eV) *m/e* 248 (100) M^+, 220 (72) $[M - C_2H_4]^+$, 206 (32) $[M - C_3H_6]^+$, 178 (35) $[M - C_3H_6N_2]^+$; IR (CsI) 3037, 1514 cm^{-1}; UV–vis (MeOH) λ_{max}, nm (ϵ) 301 (136 600), 375 (10 300), 445 sh (1600), 570 (630). Anal. Calcd for $C_{17}H_{16}N_2$: C, 82.22; H, 6.49; N, 11.28. Found: C, 81.9; H, 6.5; N, 11.3.

***N,N'*-Tetramethylene-*syn*-1,6:8,13-diimino[14]annulene (4)**: 106 mg (yield 27%) of deep-violet needles: mp 130–131 °C; ^1H NMR (CD_2Cl_2, 193 K) δ 8.44 (s, 2 H), 8.05–7.85 and 7.55–7.35 (AA'BB' system, 8 H), 0.59 (s, 4 H), 0.17 (s, 4 H); ^{13}C NMR (CD_2Cl_2, 193 K) δ 134.37, 134.02, 127.66, 120.13, 51.13, 28.34; MS (70 eV) *m/e* 262 (100) M^+, 206 (14) $[M - C_4H_8]^+$, 103 (33) $[M - C_4H_8]^{2+}$; IR (CsI) 3035, 1557, 1518 cm^{-1};

(18) Bell, F. A.; Ledwith, A.; Sherrington, D. C. *J. Chem. Soc. C* **1969**, 2719.

UV–vis (MeOH) λ_{max}, nm (ϵ) 302 (155 000), 375 (11 200), 491 (400), 580 sh (320). Anal. Calcd for $C_{18}H_{18}N_2$: C, 82.40; H, 6.92; N, 10.68. Found: C, 82.2; H, 7.0; N, 10.7.

***N,N'*-Pentamethylene-*syn*-1,6:8,13-diimino[14]annulene (5)**: 29 mg (yield 7%) of greenish-black needles: mp 112 °C; ^{1}H NMR (CD_2Cl_2, 193 K) δ 8.03 (s, 2 H), 7.77–7.74 and 7.39–7.36 (AA'BB' system, 8 H), 0.60–0.30 (m, 10 H); ^{13}C NMR (CD_2Cl_2, 193 K) δ 131.57, 131.15, 127.32, 118.17, 49.06, 27.35, 26.45; MS (70 eV) *m/e* 276 (63) M^+, 206 (37) $[M - C_5H_{10}]^+$, 103 (100) $[M - C_5H_{10}]^{2+}$; IR (CsI) 3045, 1522 cm^{-1}; UV–vis (MeOH) λ_{max}, nm (ϵ) 302 (125 900), 370 (7900), 461 (710), 613 (890).

***N,N'*-Hexamethylene-*syn*-1,6:8,13-diimino[14]annulene (6)**: 112 mg (yield 26%) of black needles: mp 163 °C; ^{1}H NMR (CD_2Cl_2) δ 7.72 (s, 2 H), 7.73–7.65 and 7.37–7.30 (AA'BB' system, 8 H), 0.67–0.42 (m, 12 H); ^{13}C NMR (CD_2Cl_2) δ 131.47, 130.24, 127.87, 118.22, 47.52, 25.35, 23.42; MS (70 eV) *m/e* 290 (3) M^+, 206 (26) $[M - C_6H_{12}]^+$, 193 (39) $[M - C_6H_{11}N]^+$, 178 (100) $[M - C_6H_{12}N_2]^+$; IR (CsI) 3051, 1565, 1522 cm^{-1}; UV–vis (MeOH) λ_{max}, nm (ϵ) 300 (123 000), 373 (8900), 435 sh (2500), 581 (1780). Anal. Calcd for $C_{20}H_{22}N_2$: C, 82.72; H, 7.64; N, 9.65. Found: C, 82.8; H, 7.5; N, 9.5.

***N,N'*-Heptamethylene-*syn*-1,6:8,13-diimino[14]annulene (7)**: 202 mg (yield 44%) of light-red needles: mp 117 °C; ^{1}H NMR (CD_2Cl_2) δ 7.53 (s, 2 H), 7.59–7.52 and 7.29–7.22 (AA'BB' system, 8 H), 0.82–0.57 (m, 14 H); ^{13}C NMR (CD_2Cl_2) δ 130.29, 129.70, 127.16, 115.18, 42.88, 25.84, 23.25, 23.01; MS (70 eV) *m/e* 304 (3) M^+, 206 (24) $[M - C_7H_{14}]^+$, 193 (20) $[M - C_7H_{13}N]^+$, 192 (16) $[M - C_7H_{14}N]^+$, 178 (100) $[M - C_7H_{14}N_2]^+$; IR (CsI) 3020, 3005, 2925, 2860, 1519 cm^{-1}; UV–vis (MeOH) λ_{max}, nm (ϵ) 302 (125 800), 369 (9800), 538 (1200). Anal. Calcd for $C_{21}H_{24}N_2$: C, 82.85; H, 7.95; N, 9.20. Found: C, 82.12; H, 8.20; N, 9.05.

***N,N'*-Perdeuteriodimethylene-*syn*-1,6:8,13-diimino[14]annulene (2-d_4), *N,N'*-2,2-dideuteriotrimethylene-*syn*-1,6:8,13-diimino[14]annulene (3-d_2), and *N,N'*-2,2,3,3-tetradeuteriotetramethylene-*syn*-1,6:8,13-diimino[14]-annulene (4-d_4)** were synthesized from the parent diimine and the respective deuteriated α,ω-dibromoalkane, i.e., 1,2-dibromoethane-d_4, 1,3-dibromo-2,2-dideuteriopropane, and 1,4-dibromo-2,2,3,3-tetradeuteriobutane, by the same procedure as that for the unlabeled compounds **2**, **3**, and **4**; they were identified by ^{1}H NMR, MS, and IR spectroscopy.

1,2-Dibromoethane-d_4 was purchased from IC Chemikalien GmbH, München.

1,3-Dibromo-2,2-dideuteriopropane was prepared according to a procedure described previously.[19]

1,4-Dibromo-2,2,3,3-tetradeuteriobutane. A solution of 1.0 g (25 mM) of $LiAlH_4$ in anhydrous ether was added dropwise to an ethereal solution of 1.263 g (7.1 mM) of diethyl succinate-d_4 (prepared from diethyl acetylenedicarboxylate; see below). The mixture was refluxed for 0.5 h and then treated with drops of water (1.5 mL) until the excess of $LiAlH_4$ was destroyed. After another 0.5 h of stirring, the mixture was acidified with 10 mL of 48% HBr; the ether as well as the most of the water was removed by rotary evaporation at 45 °C. Subsequently, another 10 mL of 48% HBr was added, along with 3 mL of concentrated sulfuric acid,[20] and the raw product was steam-distilled. Ether and aqueous sodium carbonate were added in a shaker, and the organic layer was dried with anhydrous sodium sulfate and evaporated to leave 0.985 g (yield 63%) of colorless liquid after chromatographic purification with hexane on alumina. The dibromotetradeuteriobutane was identified by ^{1}H NMR, MS, and IR spectroscopy.

Diethyl Succinate-d_4. Diethyl acetylenedicarboxylate (3.75 g, 22.1 mM) (FLUKA puriss.) in ethyl acetate was shaken with deuterium gas (CIBA-Geigy 99.9%) and a mixture of Pt/C and Pd/C catalysts. Filtration and evaporation of the organic phase yielded 1.319 g (7.41 mM) of diethyl succinate-d_4, which was purified by gas chromatography. ^{1}H NMR and MS analysis showed that the product contained about 9% of trideuterated material.

2-Bromo-*N,N'*-trimethylene-*syn*-1,6:8,13-diimino[14]annulene (3-Br). A solution of **3** (372 mg, 1.5 mmol) in dichloromethane (100 mL) was cooled to −78 °C. 2,4,4,6-Tetrabromocyclohexa-2,5-dien-1-one[21] (615 mg, 1.5 mmol) in dichloromethane (100 mL) was added under argon, and the mixture was stirred overnight. The solution was washed three times with aqueous sodium hydroxide (10%, 100 mL) and once with water. The organic phase was dried over magnesium sulfate. After evaporation of the solvent, the crude product was chromatographed with hexane on silica gel (50 × 2 cm). The first fraction was collected, and the product thus obtained was crystallized from ether, yielding **3**-Br (60 mg, 18%) as black needles (mp = 165 °C): ^{1}H NMR ($CDCl_3$) δ 9.29 (s, 1 H), 9.10 (s, 1 H), 7.82–7.13 (m, 7 H), 1.37–1.03 (m, 4 H), 0.26–0.06 (m, 2 H); ^{13}C NMR ($CDCl_3$) δ 141.70, 140.13, 134.41, 133.39, 131.78, 131.23, 130.10, 129.25, 127.25, 121.32, 121.14, 120.01, 119.86, 115.87, 49.87, 49.84, 21.88; MS (70 eV) *m/e* 328/326 (94/100) M^+, 300/298 (19/22) $[M - C_2H_4]^+$, 247 (19) $[M - Br]^+$, 219 (21) $[M - Br - C_2H_4]^+$; IR (CsI) 3033, 2928, 2839, 1513 cm^{-1}; UV–vis (CH_2Cl_2) λ_{max}, nm (ϵ) 308 (98 800), 388 (8400), 466 (1100), 576 (530).

***N,N'*-Dimethyl-*syn*-1,6:8,13-diimino[14]annulene (8).** To a solution of *syn*-1,6:8,13-diimino[14]annulene (312 mg, 1.5 mmol) in dichloromethane (50 mL) were added diisopropylethylamine (0.52 mL, 3 mmol) and trimethyloxonium tetrafluoroborate (450 mg, 3 mmol). After stirring at room temperature for 30 min, the mixture was hydrolyzed by addition of aqueous potassium carbonate (50%, 20 mL). The organic phase was washed with water and dried over magnesium sulfate. Chromatography with ether on alumina (40 × 1.5 cm) and crystallization from ether yielded **8** (284 mg, 80%) as black-red prisms (mp = 144 °C): ^{1}H NMR (CD_2Cl_2) δ 7.74 (s, 2 H), 7.61–7.56 and 7.35–7.29 (AA'BB' system, 8 H), 0.55 (s, 6 H); ^{13}C NMR (CD_2Cl_2) δ 130.63, 130.48, 127.64, 117.49, 34.46; MS (70 eV) *m/e* 236 (100) M^+, 208 (38) $[M - C_2H_4]^+$, 193 (83) $[M - C_2H_5N]^+$, 178 (90) $[M - C_2H_6N_2]^+$; IR (CsI) 3040, 1566, 1523 cm^{-1}; UV–vis (MeOH) λ_{max}, nm (ϵ) 293 (115 800), 359 (9300), 533 (760). Anal. Calcd for $C_{16}H_{16}N_2$: C, 81.32; H, 6.82; N, 11.85. Found: C, 81.3; H, 6.7; N, 11.8.

Acknowledgment. This work was supported by the Swiss National Science Foundation.

(19) Cocker, W.; Geraghty, N. W. A.; McMurry, T. B. H.; Shannon, P. V. R. *J. Chem. Soc., Perkin Trans. 1* **1984**, 2245.

(20) This method of bromination is described: *Organic Syntheses*; Wiley: New York, 1941; Collect. Vol. I, p 26 (submitted by O. Kamm and C. S. Marvel).

(21) Price, J. A. *J. Am. Chem. Soc.* **1955**, *77*, 5436.